This is an open access article published under an ACS AuthorChoice License, which permits copying and redistribution of the article or any adaptations for non-commercial purposes.

Environmental Science & Technology

Article

pubs.acs.org/est

Emissions of Ultrafine Particles and Volatile Organic Compounds from Commercially Available Desktop Three-Dimensional Printers with Multiple Filaments

Parham Azimi,[†] Dan Zhao,[†] Claire Pouzet,[†,‡] Neil E. Crain,[§] and Brent Stephens*[,†]

[†]Department of Civil, Architectural and Environmental Engineering, Illinois Institute of Technology, Chicago, Illinois 60616, United States

[‡]Ecole des Ingénieurs de la Ville de Paris, 80 Rue Rebeval, 75019 Paris, France

[§]Department of Civil, Architectural and Environmental Engineering, The University of Texas at Austin, Austin, Texas 78712, United States

Supporting Information

ABSTRACT: Previous research has shown that desktop 3D printers can emit large numbers of ultrafine particles (UFPs, particles less than 100 nm) and some hazardous volatile organic compounds (VOCs) during printing, although very few filament and 3D printer combinations have been tested to date. Here we quantify emissions of UFPs and speciated VOCs from five commercially available filament extrusion desktop 3D printers utilizing up to nine different filaments by controlled experiments in a test chamber. Median estimates of time-varying UFP emission rates ranged from $\sim 10^8$ to $\sim 10^{11}$ min^{-1} across all tested combinations, varying primarily by filament material and, to a lesser extent, bed temperature. The individual VOCs emitted in the largest quantities included caprolactam from nylon-based and imitation wood and brick filaments (ranging from ∼2 to ∼180 μg/min), styrene from acrylonitrile butadiene styrene (ABS) and high-impact polystyrene (HIPS) filaments (ranging from ∼10 to ∼110 μg/min), and lactide from polylactic acid (PLA) filaments (ranging from ∼4 to ∼5 μg/min). Results from a screening analysis of potential exposure to these products in a typical small office environment suggest caution should be used when operating many of the printer and filament combinations in poorly ventilated spaces or without the aid of combined gas and particle filtration systems.

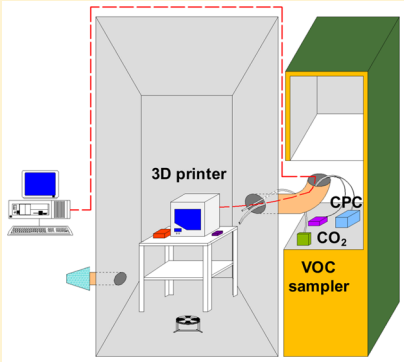

1. INTRODUCTION

Desktop three-dimensional (3D) printers are rapidly increasing in popularity. The majority of commercially available desktop 3D printers designed for the consumer market utilize an additive manufacturing technology called fused filament fabrication (FFF), also known as fused deposition modeling or molten polymer deposition. In the FFF process, a solid thermoplastic filament is forced through a heated extrusion nozzle, melted, and deposited in thin layers onto a moving bed.[1,2] A three-dimensional solid shape is formed layer-by-layer as the filament material cools and hardens. A wide variety of filament materials are now being used in desktop FFF 3D printers, including acrylonitrile butadiene styrene (ABS), poly(lactic acid) (PLA), poly(vinyl alcohol) (PVA), polycarbonate (PC), high-density polyethylene (HDPE), high-impact polystyrene (HIPS), nylon, and many other polymers, metals, ceramics, and other materials.[3] Filaments are melted at a variety of extruder nozzle temperatures and bed temperatures, and manufacturers typically recommend ranges of optimal temperatures for each filament material and thickness. ABS and PLA are currently the most commonly used filaments in desktop 3D printers, although others are also gaining popularity.[4]

It is well-known that both gases and particles are emitted during thermal processing of many thermoplastic materials.[5,6] However, little is known about the types and magnitudes of emissions from desktop FFF 3D printers and how they vary according to filament material or printer characteristics. In 2013, we published the first known measurements of emissions of ultrafine particles (UFPs: particles less than 100 nm in diameter) resulting from the operation of a single make and model of commercially available desktop FFF 3D printer using both ABS and PLA filaments.[7] These findings were crucial, as exposure to emissions from thermal decomposition of thermoplastics has been shown to have toxic effects in animals,[8−10] and exposure to UFPs from other sources has been linked to a variety of adverse human health effects.[11−17] We are aware of only one other published study to date that has investigated emissions from extrusion-based desktop 3D printers. Kim et al.[18] measured emissions of particles, total volatile organic compounds (TVOCs), several aldehydes and phthalates, and

Received: October 12, 2015
Revised: December 12, 2015
Accepted: January 7, 2016
Published: January 7, 2016

 © 2016 American Chemical Society

DOI: 10.1021/acs.est.5b04983
Environ. Sci. Technol. 2016, 50, 1260−1268

benzene, toluene, ethylbenzene, and *m*-,*p*-xylene (BTEX) from two different FFF printers operating in a small chamber, again using both ABS and PLA filaments. They confirmed that particle emissions were higher for printers utilizing ABS filaments compared to PLA filaments, and they also demonstrated higher VOC emissions from the printers using ABS filaments compared to PLA.

Despite these two studies, important gaps in our knowledge of emissions from 3D printers still remain. Only a very limited number of makes and models of printers have been tested to date, and even fewer filament materials have been characterized for gas and/or particle emissions (i.e., only ABS and PLA). Further, we hypothesize that Kim et al.[18] may have missed some individual VOCs that are emitted with some filaments because they were not specifically targeted or identified by a mass spectral library compound search. We also have no information to date on how the design or shape of printed materials, or printer characteristics such as the presence of enclosures, may influence gas and/or particle emissions.

Therefore, we advance these previous studies by quantifying emission rates of particles and a broad range of speciated VOCs from five popular commercially available desktop FFF 3D printers utilizing as many as nine different filaments to print standardized test objects in a medium-sized test chamber. We use the results to explore differences in particle and VOC emissions based on filament material and printer characteristics. We also provide preliminary data on the impact of print object geometry and the use of a partial enclosure.

2. EXPERIMENTAL METHODS

2.1. Emissions Testing Procedure. All measurements were conducted inside a 3.6 m^3 stainless steel chamber with a small stainless steel mixing fan operating as described in Supporting Information (Figure S1). Each printer was connected to a desktop computer located outside the chamber. Before each experiment began, filtered supply air was delivered to the chamber at a constant ventilation rate of approximately 1 h^{-1} for a period of at least 8 h to achieve initial steady-state background conditions. The 3D printer beds were prepared for printing before sealing the chamber by wiping with isopropyl alcohol, or, in some cases, depending on the printer and filament combination, by applying small amounts of adhesive from glue sticks following manufacturer recommendations. The printer was then powered on and began printing a small object.

For all tests but one, we printed a 10 × 10 × 1 cm standardized sample from the National Institute of Standards and Technology (NIST), as shown in Figure 1.[19] The sample was chosen because it was developed as a standardized test part to evaluate the performance of additive manufacturing technologies, and it has a range of features that were thought to potentially influence dynamic printer emissions, including a combination of solid volumes, thin protrusions, holes, and indentations. We also repeated one test with a single printer and filament combination, printing a ∼195 cm^3 cube of approximately the same printing duration as the NIST sample, allowing for an evaluation of the impact of print object shape on emissions. Nozzle and bed warm-up periods typically lasted between 5 and 10 min depending on the printer and filament, and the printing time varied from 2.5 to 4 h depending on the combination of printer, filament, and object shape.

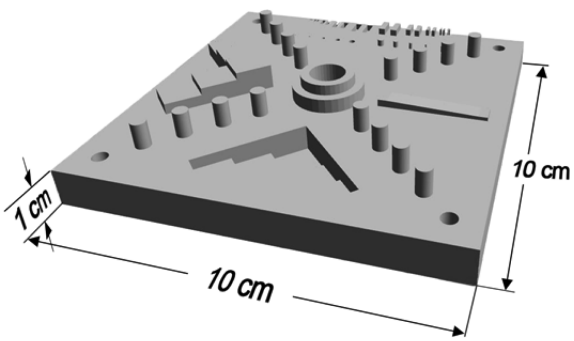

Figure 1. Shape file image of the NIST 3D printer test part used for emissions testing.

2.2. Air Sampling and Analysis. Particle concentrations were continuously measured inside the exhaust port of the chamber by use of a TSI model 3007 condensation particle counter (CPC) logging at 1 min intervals. The CPC was located inside an external exhaust hood and connected to the chamber exhaust port by a 0.9 m long piece of conductive tubing 0.6 cm in diameter. The CPC measures the total number concentrations of particles between 10 nm and 1 μm with a reported maximum concentration of $10^5/cm^3$ and a sample flow rate of 0.7 L/min. Particle concentrations were measured during all phases of the experiment, beginning with the last 45−60 min of background measurements, spanning the 2.5−4 h print period (which includes the 5−10 min warm-up phase), and ending with a final ∼3-h decay period during which particle concentrations were allowed to decrease toward background concentrations with the printer off.

We should note that although the measurement range of the CPC is 10 nm to 1 μm, the vast majority of particles emitted from most FFF printers were assumed to be in the UFP size range, as demonstrated by preliminary data in Supporting Information (Figure S4).[7,18] Thus, we consider these measurements largely representative of UFPs and use this nomenclature from here on. We periodically calibrated the CPC used for the chamber measurements via colocation measurements with a TSI model 3910 NanoScan scanning mobility particle sizer (SMPS) that had been recently calibrated by the manufacturer. We considered the SMPS to be the most accurate for UFP measurements, but it was not available for use during all of the tests. Thus, we calibrated the CPC to the SMPS using a polynomial regression from these periodic colocation experiments. The calibration between CPC particle counts and total UFP counts from the SMPS (Figure S2) was nearly linear throughout the manufacturer-reported measurement range of the CPC (up to $10^5/cm^3$) but increased exponentially beyond this range, as is typical for this instrument.[20] This was important to account for because several of the highest UFP emitters yielded raw CPC concentrations greater than $10^5/cm^3$ in the experimental chamber.

Chamber air was also sampled during the tests for VOC analysis using Tenax-GR sorbent tubes during two periods: once during the last ∼45 min prior to printing (with a printer in the chamber but not powered on or operating), and again during the last ∼45 min of printing after VOC concentrations reached approximately steady state. We used the differences in concentrations between the two samples to estimate emission rates both for speciated VOCs and for the sum of the 10 highest detectable VOCs (∑VOC). Total VOC (TVOC) concentrations inside the chamber were also continuously measured during a subset of experiments by use of a TSI Q-Trak model 7575 indoor air quality monitor with a model 982

DOI: 10.1021/acs.est.5b04983
Environ. Sci. Technol. 2016, 50, 1260−1268

photoionization detection (PID) probe to verify that TVOC concentrations achieved approximately steady state by the time air sampling for VOC analysis was conducted. These measurements were used to verify that approximately steady-state conditions were typically achieved within 2 h from the beginning of printing and that TVOC emissions followed a characteristic constant emission rate profile (Figure S3). Thus, we consider air sampling for VOC analysis during the final 45 min of printing each object reasonably representative of steady-state concentrations.

The procedure for sampling and analyzing the sorbent tubes was based on a modified version of U.S. EPA Method TO-17.[21] Sorbent tubes were inserted into a small hole in the exhaust port of the chamber and connected to a Buck VSS-1 low-flow air sampling pump located outside the chamber and operating at ~20 mL/min. Airflow rates of the sampling pumps and tubes were measured after each test by use of a Gilian Gilibrator 2 and combined with the recorded sampling duration to estimate the total air volume passed through the tubes during sampling. All sorbent tubes were shipped in a freezer pack overnight to the University of Texas at Austin and analyzed by thermal desorption followed by gas chromatography and electron ionization mass spectrometry (TD/GC/MS). An internal standard, 4-bromofluorobenzene, was used for all analysis. Individual VOCs were statistically identified and quantified by a NIST library compound search (LCS). The mass of the identified compounds was estimated from the response of the internal standard and a relative response factor of 1. The majority of the uncertainty associated with these calculations is related to the assumption that the relative response factor is 1. Relative response factors for this method have been shown to commonly range from approximately 0.75 to 1.25 for most VOCs;[22] thus we use 25% as an approximate estimate of the uncertainty in our VOC quantification method. Individual VOCs may not have the same response factors, but this provides a reasonable base estimate of the uncertainty in the reported concentrations.

We also sampled for VOCs outside the chamber during several tests. These sorbent samples were taken during the entire printing period to ensure that there were no unexpected external sources of VOCs transported into the chamber. Blank sorbent tubes were also collected outside the chamber without connecting them to the air pumps during each test to characterize adsorption of any unexpected compounds during shipping and storage. Finally, temperature and relative humidity (RH) were measured during each test with an Onset HOBO U12 data logger recording at 1 min intervals, and ventilation rates were measured during each test with CO_2 as a tracer gas. CO_2 was injected from a small tank into the chamber at the beginning of each test, and the subsequent decay of chamber CO_2 concentrations was measured by a PP Systems SBA-5 CO_2 monitor connected to an Onset HOBO U12 data logger, also recording at 1 min intervals. The ventilation rate calculation procedure is described fully in Supporting Information.

2.3. Ultrafine Particle Emission Rate Estimation. Because there was a large amount of scatter in the resulting UFP concentration data, we first applied a smoothing function to the UFP data using the "smooth" function in MATLAB R2015a, as described in Supporting Information. These smoothed concentration data were then used to estimate the time-varying UFP emission rate for each printer and filament combination via a discrete solution to a dynamic well-mixed number balance applied on the total particle number concentrations measured inside the chamber, as shown in eq 1 and derived in Supporting Information:

$$\frac{E_{\mathrm{UFP}}(t_{n+1})}{V} = \frac{[C_{\mathrm{UFP,in}}(t_{n+1}) - C_{\mathrm{UFP,in}}(t_n)]}{\Delta t} - L_{\mathrm{UFP}}\bar{C}_{\mathrm{UFP,bg}} + L_{\mathrm{UFP}}C_{\mathrm{UFP,in}}(t_n) \quad (1)$$

where $E_{\mathrm{UFP}}(t)$ is the time-varying UFP emission rate from a single 3D printer at time t (per minute), V is the chamber volume (cubic meters), $C_{\mathrm{UFP,in}}(t)$ is the UFP concentration inside the chamber at time t (per cubic meter), Δt is the time step for UFP measurements (1 min), L_{UFP} is the total UFP loss rate constant (per minute), and $\bar{C}_{\mathrm{UFP,bg}}$ is the average background UFP concentration inside the chamber prior to emissions testing. L_{UFP} was estimated from a log−linear regression with the first 60 min of data from the final decay period after printing finished, as described in Supporting Information. We should note that eq 1 makes several important assumptions that may lead to inaccuracies in estimates of UFP emission rates, such as ignoring size-resolved particle dynamics, ignoring coagulation, and assuming constant particle loss rates. Potential impacts of these assumptions are discussed in more detail in Supporting Information. We estimate the uncertainty in our time-varying UFP emission rate calculations to be approximately 45%, as described in Supporting Information.

The time-varying UFP emission rate estimates were also used to quantify the total number of UFPs emitted during printing, normalized by the mass of filament used, as shown in eq 2:

$$\dot{E}_{\mathrm{UFP}} = \frac{\sum_{k=1}^{N} E_{\mathrm{UFP}}(t_k)\Delta t}{m_{\mathrm{object}}} \quad (2)$$

where $\dot{E}_{\mathrm{UFP}}$ is the total number of UFPs emitted during printing per mass of filament used (per gram), N is the total number of time intervals during printing (minutes), and m_{object} is the mass of filament used (i.e., mass of final printed object, in grams).

2.4. Volatile Organic Compound Emission Rate Estimation. The TD/GC/MS library compound searches (LCS) identified and quantified approximately 50 speciated VOCs inside the chamber during the initial background periods and the last ~45 min of the printing periods. The emission rate of each identified VOC was estimated by use of eq 3, which assumes that ventilation was the only removal mechanism in the chamber, that the concentrations of top 10 measured emitted VOCs from 3D printers were negligible outside the chamber (verified by measurements), and that VOC concentrations achieved steady state during the final sampling period. These assumptions are discussed in more detail in Supporting Information.

$$E_{\mathrm{VOC,i}} = (C_{\mathrm{VOC,i,print}} - C_{\mathrm{VOC,i,bg}})\lambda V \quad (3)$$

$E_{\mathrm{VOC,i}}$ is the estimated constant emission rate of an individual VOC (micrograms per minute), $C_{\mathrm{VOC,i,print}}$ is the steady-state concentration of an individual VOC inside the chamber during the last ~45 min of printing (micrograms per cubic meter), and $C_{\mathrm{VOC,i,bg}}$ is the background concentration of an individual VOC inside the chamber prior to printing (micrograms per cubic meter). We estimate the uncertainty in our speciated VOC emission rate calculations to be approximately 36%, as described in Supporting Information.

The emission rate of each printer for the sum of the 10 highest detectable VOCs ($\sum$VOC) was estimated by adding all positive individual VOC emission rates of the top 10

DOI: 10.1021/acs.est.5b04983
Environ. Sci. Technol. 2016, 50, 1260−1268

Table 1. Summary of All Experiments[a]

printer	filament	extruder temp (°C)	bed temp (°C)	bed prep	mass (g)	enclosure	printing duration
FlashForge Creator	ABS white	200	110	glue	40.2	no	3 h 42 min
	PLA red	200	110	glue	53.2	no	3 h 42 min
Dremel 3D Idea Builder	PLA white[b,c]	230	room temperature	alcohol wipe	55.2	yes	2 h 49 min
XYZprinting da Vinci 1.0	ABS blue	230	100	glue	40.4	yes	2 h 26 min
LulzBot Mini	ABS red[b,c,d]	240	110	alcohol wipe	44.5	no	2 h 33 min
	ABS red[e]	240	110	alcohol wipe	56.7	no	2 h 42 min
	PLA red	190	45	alcohol wipe	53.1	no	3 h 25 min
	HIPS black[b]	240	100	alcohol wipe	47.4	no	2 h 28 min
	nylon bridge semitransparent	230	65	glue	46.5	no	2 h 55 min
	laybrick white	200	65	alcohol wipe	57.7	no	3 h 0 min
	laywood brown	200	65	alcohol wipe	48.3	no	3 h 2 min
	polycarbonate transparent[b]	270	110	glue	52.1	no	2 h 38 min
	PCTPE semitransparent	235	65	glue	47.8	no	3 h 2 min
	T-Glase transparent red	240	60	alcohol wipe	49.4	no	3 h 2 min
MakerBot Replicator 2X	ABS white[d]	230	110	glue	40.3	yes	2 h 38 min
	ABS white[d]	230	110	glue	40.7	no	2 h 38 min

[a]For all tests but one, we printed a 10 × 10 × 1 cm standardized sample from NIST. [b]Experimental conditions with duplicate VOC emissions tests. [c]Experimental conditions with duplicate UFP emissions tests. [d]Experiments with simultaneous VOC sampling conducted outside the chamber. [e]In this case we printed a ∼195 cm^3 cube with approximately the same printing duration as the NIST sample.

compounds with the highest concentrations inside the chamber during the last 45 min of the printing period. We limited to the top 10 highest concentration compounds because compounds below the top 10 added negligible amounts to the overall detectable $\sum VOC_i$ mass. We also normalized $\sum VOC$ emission rates by the mass of filament consumed by use of eq 4:

$$\dot{E}_{\sum VOC} = \frac{\sum_{k=1}^{N} E_{\sum VOC}(t_k)\Delta t}{m_{object}} \quad (4)$$

where $E_{\sum VOC}$ is the total VOC emission rate of a printer for the top 10 identified compounds and $\dot{E}_{\sum VOC}$ is the total VOC emission rate per mass of filament used (micrograms per gram).

2.5. Printer and Filament Descriptions. We characterized UFP and VOC emissions from a total of 16 unique combinations of printers and filaments, including five popular commercially available makes and models of desktop 3D printers with up to nine different filament materials. The five printers included (1) a FlashForge Creator dual extruder model compatible with ABS and PLA (both filaments were tested); (2) a Dremel 3D Idea Builder compatible with PLA only; (3) an XYZprinting da Vinci 1.0 compatible with ABS only; (4) a MakerBot Replicator 2X compatible with ABS only; and (5) a LulzBot Mini that was compatible with many different types of filaments. The LulzBot printer was tested with nine different filaments that are commonly used, including ABS, PLA, high-impact polystyrene (HIPS), semitransparent nylon, laybrick (an imitation brick material of unknown chemical composition), laywood (an imitation wood material of unknown chemical composition), transparent polycarbonate, a semitransparent nylon-based plasticized copolyamide thermoplastic elastomer (PCTPE), and a transparent polyester resin filament called T-Glase. The Dremel, XYZprinting, and MakerBot printers all had built-in plastic enclosures surrounding the apparatus (although they were not airtight), while the FlashForge and LulzBot did not have any enclosures. This list of printers is not meant to be exhaustive, but it is designed to span a reasonable range of currently popular printers with relatively generalizable characteristics such as filament type, nozzle and bed temperatures, and the presence or absence of a partial enclosure. Table 1 summarizes all experiments that were conducted.

Fifteen of the 16 printer and filament combinations were used to print the NIST test part, while one test combination (LulzBot-ABS) was also used to print a cube. The MakerBot with ABS filament was also tested twice: once with the plastic enclosure from the manufacturer installed as received from the factory and once with the enclosure intentionally removed. We also performed duplicate VOC measurements for four printer and filament combinations and two duplicate UFP measurements to evaluate the repeatability of our experiments.

3. RESULTS AND DISCUSSION

3.1. Ultrafine Particle Emission Rates. Figure 2a shows an example of time-varying UFP concentrations resulting from just one test of one of the printers with ABS filament (LulzBot Mini), along with the smoothed fit to the UFP concentration data. The left guideline in Figure 2a shows the moment that printers began warming up prior to printing, which we considered part of the printing emissions period. Figure 2b shows the time-varying UFP emission rates estimated from eq 1. Figures S6−S23 show similar time-series profiles of both UFP concentrations and emission rates for all 16 experimental combinations, as well as two duplicates.

Results in Figure 2a are similar to results from most of the experiments in that UFP concentrations typically rapidly increased just after printing began and persisted for the first 10−20 min, then decreased to a lower level, albeit typically to a level that was still higher than the background concentration. During some tests with other printer and filament combinations, UFP concentrations peaked again near the end of the print period as the thin protrusions on the printed object were

DOI: 10.1021/acs.est.5b04983
Environ. Sci. Technol. 2016, 50, 1260−1268

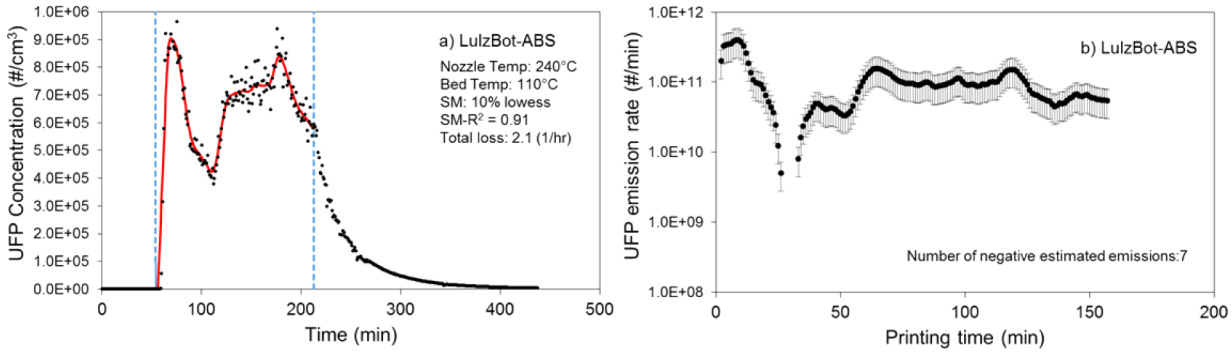

Figure 2. (a) Calibrated and smoothed UFP concentrations and (b) estimates of time-varying UFP emission rates for one sample test condition with LulzBot Mini 3D printer and ABS filament. SM refers to the data smoothing method utilized.

created. However, the magnitude and shape of dynamic UFP concentrations varied widely depending on the printer, filament, shape of printed object, and nozzle and bed temperatures. In a few scenarios (e.g., Figure 2a), UFP concentrations reached an approximate steady-state level toward the end of printing period. We used data from these periods to verify that the discretized time-varying emission rate calculation method (eq 1) also yielded similar estimates of UFP emission rates as the simple steady-state solution to the mass balance, as described in Supporting Information. Results from both solution methods were in good agreement for these periods, suggesting that the dynamic solution method provides reasonable emission rate estimates.

Figure 3 shows the range of time-varying UFP emission rates estimated for all 16 printer and filament combinations, grouped by (i) ABS filaments, (ii) PLA filaments, and (iii) all filaments other than ABS or PLA.

UFP emission rates varied substantially depending on make and model of the printer, type of filament material, nozzle and bed temperatures, and time of printing. The highest UFP emission rates typically occurred with the printers utilizing ABS filaments, with median values ranging from $\sim 2 \times 10^{10}$ to $\sim 9 \times 10^{10}$ min^{-1} across all ABS printers with or without enclosures. The lowest UFP emission rates occurred with the three printers

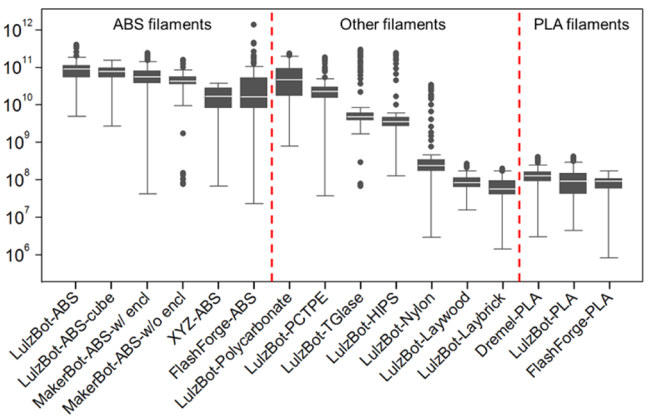

Figure 3. Summary of time-varying UFP emission rates estimated for 16 3D printer and filament combinations. Each data point represents data from 1 min intervals, and the combination of data points represents the entire printing period (typically between 2.5 and 4 h). Boxes show the 25th and 75th percentile values with the 50th percentile (median) in between. Whiskers represent upper and lower adjacent values, and circles represent outliers beyond those values.

utilizing PLA filaments, regardless of printer make and model, with median UFP emission rates of $\sim 10^8$ min^{-1}. This is lower than what we estimated in our original study with a different make and model printer as well as a different study design[7] but is similar to other recent chamber tests.[18] Median UFP emission rates for other filaments were highest for polycarbonate filament ($\sim 4 \times 10^{10}$ min^{-1}), followed by PCTPE ($\sim 2 \times 10^{10}$ min^{-1}), T-Glase ($\sim 5 \times 10^9$ min^{-1}), HIPS ($\sim 4 \times 10^9$ min^{-1}), nylon ($\sim 2 \times 10^8$ min^{-1}), laywood ($\sim 8 \times 10^7$ min^{-1}), and laybrick ($\sim 6 \times 10^7$ min^{-1}), all printed with the LulzBot Mini printer.

Printing a cube instead of the NIST test part with ABS filament (in the LulzBot printer) did not meaningfully alter the magnitude of UFP emission rates, although it did slightly change the time-varying shape of the UFP emissions profile (Figure S8). Interestingly, the presence of an enclosure only moderately reduced UFP emission rates from the MakerBot–ABS combination, with a ~35% reduction in the median emission rate (although this variation is within the estimate of uncertainty). Larger reductions were not observed, perhaps because the enclosure was not completely sealed and large gaps were visible. While these two comparisons provide preliminary data on how printed shape and presence of an enclosure may impact particle emissions from 3D printers, no other definitive conclusions can be drawn given this limited data set. Finally, data from two sets of duplicate tests (Figures S6 and S7and Figures S17 and S18) also demonstrated that there is some inherent variability in UFP emissions between repeated tests, as median emission rate estimates from these comparisons were within 57% and 48% of each other, respectively.

3.2. Volatile Organic Compound Emission Rates.

Figure 4 summarizes estimates of individual speciated VOC and ∑VOC emission rates from each of the 16 printer and filament combinations. Only the top three speciated VOCs with the highest concentrations measured in each test are shown individually, while the remaining top 10 individual VOCs are summarized as other VOCs. The sum of these yields an estimate of the ∑VOC emission rate. We also provide a list of the top 10 individual VOCs with the highest measured concentrations during the printing periods for all 16 experimental combinations inside the chamber and four duplicate experiments for VOC sampling in Table S2, as well as during four periods of VOC sampling outside the chamber in Table S3.

Filament material drove the majority of differences in the types of VOCs emitted, while printer make and model drove the majority of differences in the overall mass of VOCs emitted

DOI: 10.1021/acs.est.5b04983
Environ. Sci. Technol. 2016, 50, 1260−1268

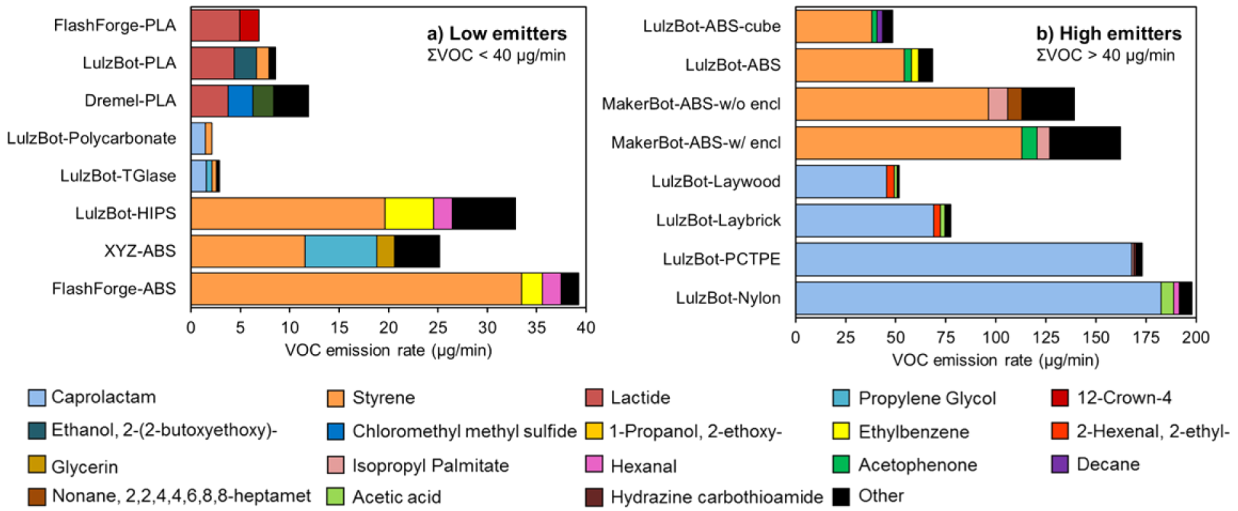

Figure 4. Estimates of emission rates for the top three highest-concentration VOCs as well as sum of the top 10 detectable VOCs (∑VOC) resulting from operation of 16 3D printer and filament combinations. The figure is divided into (a) low emitters, with $E_{\sum VOC} < 40$ μg/min, and (b) high emitters, with $E_{\sum VOC} > 40$ μg/min, for visual clarity. Note that although no error bars are shown in the figure, we estimate the uncertainty in each individual VOC emission rate to be ∼36% as described in Supporting Information.

with the same filament. Estimates of total VOC emission rates ($E_{\sum VOC}$) ranged from as low as ∼3 μg/min for the polycarbonate filament to nearly 200 μg/min for the nylon filament (both printed with the LulzBot). The top three highest emitted compounds accounted for at least 70% of ∑VOC emissions in all cases. For most of the printer and filament combinations, a single VOC dominated the ∑VOC emissions.

The primary individual VOC emitted from all six ABS filament and printer combinations and the only HIPS filament tested was styrene. Estimates of styrene emission rates with these filaments ranged from ∼12 to ∼113 μg/min, depending on the printer make and model. Interestingly, both the lowest and highest styrene emission rates were measured for printers with a partial enclosure (XYZprinting and MakerBot). Both styrene and total VOC emission rates were slightly lower when the LulzBot−ABS combination printed a cube compared to the standard NIST test part, but they were actually slightly higher for the MakerBot−ABS combination with the plastic enclosure compared to results without the enclosure.

The primary individual VOC emitted from nylon, PCTPE, laybrick, and laywood filaments was caprolactam. All of these filaments were installed in the LulzBot printer and all were classified as high emitters in Figure 4b, with caprolactam emission rates as high as ∼180 μg/min for the nylon filament. Caprolactam was also emitted from the polycarbonate and T-Glase filaments installed in the LulzBot printer, albeit at much lower levels (Figure 4a). Finally, the primary individual VOC emitted from PLA filaments was lactide (1,4-dioxane-2,5-dione, 3,6-dimethyl), albeit in relatively low quantities, with emission rates ranging from ∼4 to ∼5 μg/min in the three printers using PLA filaments. We are confident that the majority of the identified VOCs originated from the filament materials for most of the printer tests, even for the tests that had glue applied to the bed, because the main components measured during the glue-only test (propylene glycol and glycerin, as shown in Table S2) were found only in one filament/printer combination in Figure 4.

3.3. Impacts of Nozzle and Bed Temperatures. Next, we explored our estimates of both UFP and ∑VOC emission rates as a function of both nozzle and bed temperatures (Figure 5). The mean UFP and ∑VOC emission rates are split into three groups of bed temperature (less than 45, 60−65, and 100−110 °C) and plotted versus nozzle temperature (which varied from 190 to 270 °C, as described in Table 1).

Nozzle temperatures did not have a large influence on UFP emission rates from this set of printers at either low or high bed temperatures. However, nozzle temperatures did appear to influence UFP emission rates at midrange bed temperatures, as UFP emission rates were higher with increased nozzle temperatures. More importantly, bed temperatures alone appeared to influence UFP emission rates in this sample of printers. Most of the printer/filament combinations with the highest bed temperatures had the highest UFP emission rates, while most of the printer/filament combinations with the lowest bed temperatures had the lowest UFP emission rates. There was no apparent relationship observed between ∑VOC emission rates and either bed or nozzle temperatures across this sample of printers and filaments. However, we should note that with this limited sample size, these relationships are only considered suggestive.

3.4. Correlations between Total Ultrafine Particle and Sum of Volatile Organic Compound Emissions per Mass of Filament. Figure 6 compares the total number of UFPs emitted (eq 2) and the ∑VOC mass emitted (eq 4) during printing, normalized by the mass of filament, for each of the 16 primary printer and filament combinations.

The total number of UFPs emitted per gram of filament printed ranged from a minimum of $\sim 2 \times 10^8$ g^{-1} for the LulzBot−laybrick combination to a maximum of over 2×10^{11} g^{-1} for multiple printers with ABS filaments. The ∑VOC mass emitted per gram of filament printed ranged from a minimum of ∼6 μg/g for the LulzBot−polycarbonate combination to nearly 800 μg/g for the LulzBot−nylon combination. In general, ABS, PCTPE, and HIPS filaments had high mass-normalized emission rates of both UFPs and ∑VOCs, while PLA filaments had relatively low mass-normalized UFP and ∑VOC emission rates. Interestingly, both T-Glase and polycarbonate filaments (both used in the LulzBot printer) had low ∑VOC emissions but high UFP emissions. Conversely, both laywood and laybrick filaments (also used

DOI: 10.1021/acs.est.5b04983
Environ. Sci. Technol. 2016, 50, 1260−1268

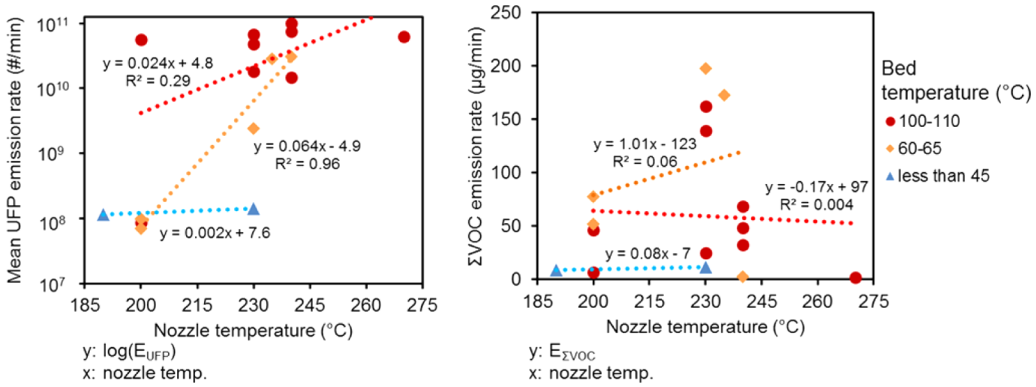

Figure 5. Impact of nozzle and bed temperature on mean UFP and TVOC emission rates.

in the LulzBot printer) had relatively high ∑VOC emission rates but low UFP emission rates. These data suggest that filament material selection drives both UFP and ∑VOC emissions, although knowledge of one type of emissions may not necessarily be used to predict the other.

3.5. Implications for Human Exposure and Health Effects. Measurements of UFP and individual VOC emission rates presented here have important implications for human exposure and health effects. For example, styrene, which is classified as a possible human carcinogen by the International Agency for Research on Cancer (IARC classification group 2B),[23] was emitted in large amounts by all ABS filaments and the one HIPS filament. Caprolactam was also emitted in large amounts by four of the filaments: nylon, PCTPE, laybrick, and laywood. Although caprolactam is classified as probably not carcinogenic to humans,[24] the California Office of Environmental Health Hazard Assessment (OEHHA) maintains acute, 8-h, and chronic reference exposure levels (RELs) of only 50, 7, and 2.2 $\mu g/m^3$, respectively.[25] We are not aware of any relevant information regarding the inhalation toxicity of lactide, the primary individual VOC emitted from PLA filaments.

To provide a basis for comparison to regulatory exposure limits and to help understand potential implications for human health, we used these estimates of UFP and individual VOC emission rates to predict steady-state concentrations that would likely result from constant printer operation in a typical small well-mixed office environment. This effort is not meant to serve as a detailed exposure model but rather as a screening analysis for potential health implications. We should also note that this analysis does not take into account proximity effects that could serve to substantially elevate exposures to both UFPs and VOCs in certain microenvironments compared to well-mixed conditions.

Let us assume that one desktop 3D printer operates continuously in a well-mixed 45 m^3 furnished and conditioned office space (i.e., the same office space reported by Stephens et al.[7] Let us assume a worst-case scenario in which a single printer has the maximum median UFP and individual VOC emission rates from the findings herein, which include ~10^{11} min^{-1} for UFPs, 183 $\mu g/min$ for caprolactam, 113 $\mu g/min$ for styrene, and 5 $\mu g/min$ for lactide. Let us assume a typical office ventilation rate of 1 h^{-1},[26] no sorption losses for the three VOCs (likely a conservative estimate),[27,28] and a typical UFP deposition loss rate constant of 1.3 h^{-1}.[29] Under these conditions, steady-state indoor concentrations of each of these constituents would be elevated to ~58 000 cm^{-3} for UFPs, ~244 $\mu g/m^3$ for caprolactam, ~150 $\mu g/m^3$ for styrene, and ~6 $\mu g/m^3$ for lactide.

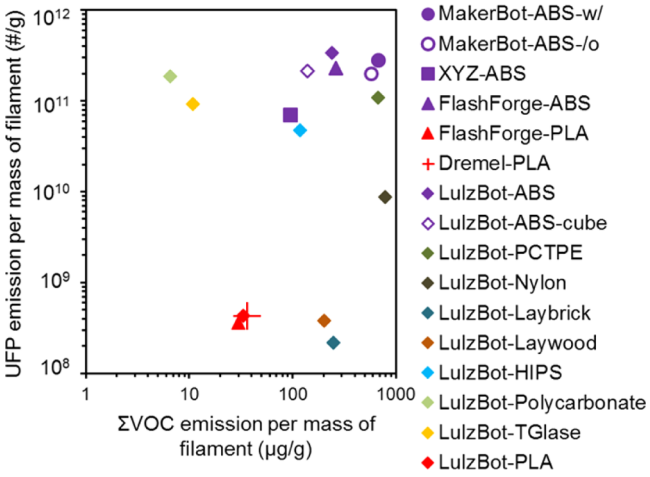

Figure 6. Comparison of total UFP and TVOC emissions per mass of filament.

The predicted caprolactam concentration (244 $\mu g/m^3$) would exceed all three RELs identified by the California OEHHA,[25] which suggests that although there is considerable uncertainty in this estimate, exposure to caprolactam from desktop 3D printing in a typical office environment with nylon and nylon-based filaments could lead to adverse health outcomes, particularly for susceptible individuals. Acute exposure to high concentrations of caprolactam is known to be "irritating to the eyes and the respiratory tract" and "may cause effects on the central nervous system", according to the Centers for Disease Control and Prevention (CDC).[30]

The predicted styrene concentration in this configuration (150 $\mu g/m^3$) would be approximately 20 times higher than the highest styrene concentration measured in commercial buildings in the U.S. EPA BASE study[31] and more than 20 times higher than the average concentration in U.S. residences.[32] There are also reports that suggest exposure to styrene at these concentrations could be problematic for human health. For example, high indoor styrene concentrations have been estimated to yield relatively high lifetime cancer risks in previous studies that assumed typical potency factors,[33] and even moderate styrene concentrations (i.e., greater than only 2 $\mu g/m^3$) have been associated with elevated risk of pulmonary infections in infants.[34]

Although we are not aware of any regulatory limits for indoor UFP concentrations, an increase in UFP concentrations to

DOI: 10.1021/acs.est.5b04983
Environ. Sci. Technol. 2016, 50, 1260−1268

~58 000 cm^{-3} would be approximately 10 times higher than what we typically observe in indoor air in our office and laboratory environments and what has been reported as a typical 8-h average indoor concentration in schools.[35] However, it would only be moderately higher than typical time-averaged concentrations in homes[36] but lower than what is often observed in other microenvironments.[37]

Given these findings, we are prompted to make the following recommendations. First, additional measurements should be conducted to more accurately quantify personal exposures to both UFPs and speciated VOCs that account for proximity effects presented by typical 3D printer use patterns. Second, manufacturers should work toward designing low-emitting filament materials and/or printing technologies. Third, in the absence of new low-emitting filaments, manufacturers should work to evaluate the effectiveness of sealed enclosures on both UFP and VOC emissions or to introduce combined gas and particle filtration systems. Until then, we continue to suggest that caution should be used when operating many printer and filament combinations in enclosed or poorly ventilated spaces or without the aid of gas and particle filtration systems. This is particularly true for both styrene- and nylon-based filaments, based on data from the relatively large sample of printers and filament combinations evaluated here.

■ ASSOCIATED CONTENT

Supporting Information

The Supporting Information is available free of charge on the ACS Publications website at DOI: 10.1021/acs.est.5b04983.

Additional text, 23 figures, and four tables with descriptions of solution methods, experimental setup details, calibrations, uncertainty analysis, and all resulting UFP and VOC data (PDF)

■ AUTHOR INFORMATION

Corresponding Author

*Phone (312) 567-3356; e-mail brent@iit.edu.

Notes

The authors declare no competing financial interest.

■ ACKNOWLEDGMENTS

This research was funded by the Centers for Disease Control and Prevention through the National Institute for Occupational Safety and Health (Grant ROH010699). Its contents are solely the responsibility of the authors and do not necessarily represent the official views of the Centers for Disease Control and Prevention or the Department of Health and Human Services.

■ REFERENCES

(1) Getting Started with a 3D Printer. *2013 MAKE Ultimate Guide to 3D Printing*; http://makezine.com/2012/11/13/getting-started-with-a-3d-printer/.

(2) Gross, B. C.; Erkal, J. L.; Lockwood, S. Y.; Chen, C.; Spence, D. M. Evaluation of 3D Printing and Its Potential Impact on Biotechnology and the Chemical Sciences. *Anal. Chem.* **2014**, *86* (7), 3240−3253.

(3) *MatterHackers 3D printer filament comparison guide*, 2015; https://www.matterhackers.com/3d-printer-filament-compare.

(4) Ragan, S. Plastics for 3D Printing. *2013 MAKE Ultimate Guide To 3D Printing*, Winter **2013**; page 22; http://makezine.com/2012/11/13/plastics-for-3d-printing/.

(5) Contos, D. A.; Holdren, M. W.; Smith, D. L.; Brooke, R. C.; Rhodes, V. L.; Rainey, M. L. Sampling and Analysis of Volatile Organic Compounds Evolved During Thermal Processing of Acrylonitrile Butadiene Styrene Composite Resins. *J. Air Waste Manage. Assoc.* **1995**, *45* (9), 686−694.

(6) Unwin, J.; Coldwell, M. R.; Keen, C.; McAlinden, J. J. Airborne Emissions of Carcinogens and Respiratory Sensitizers during Thermal Processing of Plastics. *Ann. Occup. Hyg.* **2013**, *57* (3), 399−406.

(7) Stephens, B.; Azimi, P.; El Orch, Z.; Ramos, T. Ultrafine particle emissions from desktop 3D printers. *Atmos. Environ.* **2013**, *79*, 334−339.

(8) Zitting, A.; Savolainen, H. Effects of single and repeated exposures to thermo-oxidative degradation products of poly-(acrylonitrile-butadiene-styrene) (ABS) on rat lung, liver, kidney, and brain. *Arch. Toxicol.* **1980**, *46* (3−4), 295−304.

(9) Schaper, M. M.; Thompson, R. D.; Detwiler-Okabayashi, K. A. Respiratory Responses of Mice Exposed to Thermal Decomposition Products from Polymers Heated at and Above Workplace Processing Temperatures. *Am. Ind. Hyg. Assoc. J.* **1994**, *55* (10), 924−934.

(10) Oberdorster, G.; Oberdorster, E.; Oberdorster, J. Nanotoxicology: An Emerging Discipline Evolving from Studies of Ultrafine Particles. *Environ. Health Perspect.* **2005**, *113* (7), 823−839.

(11) Oberdörster, G.; Sharp, Z.; Atudorei, V.; Elder, A.; Gelein, R.; Kreyling, W.; Cox, C. Translocation of Inhaled Ultrafine Particles to the Brain. *Inhalation Toxicol.* **2004**, *16* (6−7), 437−445.

(12) Oberdörster, G.; Celein, R. M.; Ferin, J.; Weiss, B. Association of Particulate Air Pollution and Acute Mortality: Involvement of Ultrafine Particles? *Inhalation Toxicol.* **1995**, *7* (1), 111−124.

(13) Delfino, R. J.; Sioutas, C.; Malik, S. Potential role of ultrafine particles in associations between airborne particle mass and cardiovascular health. *Environ. Health Perspect.* **2005**, *113* (8), 934−946.

(14) HEI. *Understanding the Health Effects of Ambient Ultrafine Particles*; HEI Review Panel on Ultrafine Particles; HEI Perspectives 3; Health Effects Institute: Boston, MA, 2013; http://pubs.healtheffects.org/getfile.php?u=893.

(15) Weichenthal, S.; Dufresne, A.; Infante-Rivard, C. Indoor ultrafine particles and childhood asthma: exploring a potential public health concern. *Indoor Air* **2007**, *17* (2), 81−91.

(16) Stölzel, M.; Breitner, S.; Cyrys, J.; Pitz, M.; Wölke, G.; Kreyling, W.; Heinrich, J.; Wichmann, H.-E.; Peters, A. Daily mortality and particulate matter in different size classes in Erfurt, Germany. *J. Exposure Sci. Environ. Epidemiol.* **2007**, *17* (5), 458−467.

(17) Andersen, Z. J.; Olsen, T. S.; Andersen, K. K.; Loft, S.; Ketzel, M.; Raaschou-Nielsen, O. Association between short-term exposure to ultrafine particles and hospital admissions for stroke in Copenhagen, Denmark. *Eur. Heart J.* **2010**, *31* (16), 2034−2040.

(18) Kim, Y.; Yoon, C.; Ham, S.; Park, J.; Kim, S.; Kwon, O.; Tsai, P.-J. Emissions of Nanoparticles and Gaseous Material from 3D Printer Operation. *Environ. Sci. Technol.* **2015**, *49*, 12044−12053.

(19) Moylan, S.; Slotwinski, J.; Cooke, A.; Jurrens, K.; Donmez, M. A. Proposal for a standardized test artifact for additive manufacturing machines and processes. *Solid Freeform Fabr. Symp. Proc.* **2012**, 6−8, http://sffsymposium.engr.utexas.edu/Manuscripts/2012/2012-69-Moylan.pdf.

(20) Westerdahl, D.; Fruin, S.; Sax, T.; Fine, P. M.; Sioutas, C. Mobile platform measurements of ultrafine particles and associated pollutant concentrations on freeways and residential streets in Los Angeles. *Atmos. Environ.* **2005**, *39* (20), 3597−3610.

(21) U.S. EPA. Compendium Method TO-17: Determination of Volatile Organic Compounds in Ambient Air Using Active Sampling Onto Sorbent Tubes. In *Compendium of Methods for the Determination of Toxic Organic Compounds in Ambient Air*, 2nd ed.; EPA/625/R-96/010b; U.S. Environmental Protection Agency, 1999; http://www3.epa.gov/ttnamti1/files/ambient/airtox/to-17r.pdf.

(22) Allgood, C.; Orlando, R.; Munson, B. Correlations of relative sensitivities in gas chromatography electron ionization mass spectrometry with molecular parameters. *J. Am. Soc. Mass Spectrom.* **1990**, *1* (5), 397−404.

DOI: 10.1021/acs.est.5b04983
Environ. Sci. Technol. 2016, 50, 1260−1268

(23) IARC. *Some Traditional Herbal Medicines, Some Mycotoxins, Naphthalene and Styrene*; IARC Monographs on the Evaluation of Carcinogenic Risks to Humans, Vol. *82*; International Agency for Research on Cancer, 2002; http://monographs.iarc.fr/ENG/Monographs/vol82/mono82.pdf.
(24) IARC. *Re-evaluation of Some Organic Chemicals, Hydrazine and Hydrogen Peroxide*; IARC Monographs on the Evaluation of Carcinogenic Risks to Humans, Vol. *71*; International Agency for Research on Cancer, 1999; http://monographs.iarc.fr/ENG/Monographs/vol71/mono71.pdf.
(25) Office of Environmental Health Hazard Assessment. Table of All OEHHA Acute, Chronic and 8 h Reference Exposure Levels; http://oehha.ca.gov/air/allrels.html (accessed October 7, 2015).
(26) Bennett, D.; Apte, M.; Wu, X.; Trout, A.; Faulkner, D.; Maddalena, R.; Sullivan, D. *Indoor environmental quality and heating, ventilating, and air conditioning survey of small and medium size commercial buildings*; CEC-500-2011-043; California Energy Commission: 2011; http://www.energy.ca.gov/2011publications/CEC-500-2011-043/CEC-500-2011-043.pdf.
(27) Singer, B. C.; Revzan, K. L.; Hotchi, T.; Hodgson, A. T.; Brown, N. J. Sorption of organic gases in a furnished room. *Atmos. Environ.* **2004**, *38* (16), 2483−2494.
(28) Singer, B. C.; Hodgson, A. T.; Hotchi, T.; Ming, K. Y.; Sextro, R. G.; Wood, E. E.; Brown, N. J. Sorption of organic gases in residential rooms. *Atmos. Environ.* **2007**, *41* (15), 3251−3265.
(29) Wallace, L.; Kindzierski, W.; Kearney, J.; MacNeill, M.; Héroux, M.-È.; Wheeler, A. J. Fine and Ultrafine Particle Decay Rates in Multiple Homes. *Environ. Sci. Technol.* **2013**, *47* (22), 12929−12937.
(30) CDC. The National Institute for Occupational Safety and Health (NIOSH) International Chemical Safety Cards (ICSC), Caprolactam; Centers for Disease Controls and Prevention, 1994; http://www.cdc.gov/niosh/ipcsneng/neng0118.html.
(31) Girman, J. R.; Hadwen, G. E.; Burton, L. E.; et al. Individual Volatile Organic Compound Prevalence and Concentrations in 56 Buildings of the Building Assessment Survey and Evaluation (BASE) Study. *Proc. Indoor Air* **1999**, Vol. *II*, pp 460−465; http://www.epa.gov/sites/production/files/2014-08/documents/base_2_460.pdf.
(32) Logue, J. M.; Price, P. N.; Sherman, M. H.; Singer, B. C. A method to estimate the chronic health impact of air pollutants in U.S. residences. *Environ. Health Perspect.* **2012**, *120* (2), 216−222.
(33) Guo, H.; Lee, S. C.; Chan, L. Y.; Li, W. M. Risk assessment of exposure to volatile organic compounds in different indoor environments. *Environ. Res.* **2004**, *94* (1), 57−66.
(34) Diez, U.; Kroessner, T.; Rehwagen, M.; Richter, M.; Wetzig, H.; Schulz, R.; Borte, M.; Metzner, G.; Krumbiegel, P.; Herbarth, O. Effects of indoor painting and smoking on airway symptoms in atopy risk children in the first year of life results of the LARS-study. Leipzig Allergy High-Risk Children Study. *Int. J. Hyg. Environ. Health* **2000**, *203* (1), 23−28.
(35) Diapouli, E.; Chaloulakou, A.; Spyrellis, N. Levels of ultrafine particles in different microenvironments–implications to children exposure. *Sci. Total Environ.* **2007**, *388* (1−3), 128−136.
(36) Bhangar, S.; Mullen, N. A.; Hering, S. V.; Kreisberg, N. M.; Nazaroff, W. W. Ultrafine particle concentrations and exposures in seven residences in northern California. *Indoor Air* **2011**, *21*, 132−144.
(37) Wallace, L.; Ott, W. Personal exposure to ultrafine particles. *J. Exposure Sci. Environ. Epidemiol.* **2011**, *21* (1), 20−30.

DOI: 10.1021/acs.est.5b04983
Environ. Sci. Technol. 2016, 50, 1260−1268